AGU PUBLICATIONS

Geophysical Research Letters

RESEARCH LETTER
10.1002/2016GL068524

**Key Points:**
- We study the relationship between changes in seismicity rate and aseismic slip for the Boso area
- We propose an objective measure of the seismicity rate directly associated with changes in slip rate
- We show an increase of the background seismicity explaining the shortening of the SSEs occurrence

**Supporting Information:**
- Supporting Information S1

**Correspondence to:**
T. Reverso,
thomas.reverso@adelaide.edu.au

**Citation:**
Reverso, T., D. Marsan, A. Helmstetter, and B. Enescu (2016), Background seismicity in Boso Peninsula, Japan: Long-term acceleration, and relationship with slow slip events, *Geophys. Res. Lett.*, *43*, 5671–5679, doi:10.1002/2016GL068524.

Received 12 NOV 2015
Accepted 12 MAY 2016
Accepted article online 17 MAY 2016
Published online 4 JUN 2016



# Background seismicity in Boso Peninsula, Japan: Long-term acceleration, and relationship with slow slip events

**T. Reverso[1,2,3], D. Marsan[1,2], A. Helmstetter[2,4], and B. Enescu[5]**

[1]ISTerre, Université de Savoie Mont Blanc, Le Bourget-du-Lac, France, [2]CNRS, ISTerre, Le Bourget-du-Lac, France, [3]Now at School of Physical Sciences, University of Adelaide, SA, Australia, [4]ISTerre, Université Grenoble-Alpes, Grenoble, France, [5]Department of Geophysics, Graduate School of Science, Kyoto University Kitashirakawa, Oiwake-cho, Sakyo-ku, Kyoto, Japan

**Abstract** Slow slip events (SSEs) in subduction zones can trigger earthquake swarms, especially at shallow depth. The monitoring of seismicity rates has therefore the potential to help detect and characterize SSEs, and transient changes in coupling. However, the relationship between seismicity rate and slow slip rate during a SSE is unknown and made complicated by aftershock triggering within the swarm. Here we propose to complement geodetic methods with an objective measure of the seismicity rate that is directly associated with changes in slip rate. We show that this measure, applied to known occurrences of SSEs in the Boso area, Japan, yields an estimate, albeit indirect, of their seismic moment, hence their slip rate. We finally prove that the background rate in Boso has been accelerating since 1990; this explains previous observations of the shortening of the recurrence time between SSEs in Boso, that clearly predate the 2011 $M_w$9.0 Tohoku-Oki earthquake.

## 1. Introduction

Episodes of slow, aseismic slip on faults can trigger earthquakes, as found in the Hikuarangi subduction zone [*Delahaye et al.*, 2009], in Ecuador [*Vallée et al.*, 2013], or in Cascadia [*Vidale et al.*, 2011]. In Mexico, *Liu et al.* [2007] noted increases in seismicity during slow slip events (SSEs) in 1998, 2001 – 2002 and 2006. At the Kilauea volcano, seismic swarms have systematically occurred during slow slip marking the destabilization of the southeast flank of the volcano [*Montgomery-Brown et al.*, 2009, 2011, 2013]. The rapid anomalous increase of earthquake rate can therefore reveal slow deformation transients associated with slow aseismic slip, as long as these transients occur in seismicity-prone areas, and at shallow depth [*Delahaye et al.*, 2009]. The detection of SSEs, particularly in subduction zones, is thus potentially feasible by monitoring changes in seismicity that depart from a normal behavior.

Methods have been proposed to detect seismic swarms in a systematic manner that permit this monitoring. *Holtkamp and Brudzinski* [2011] produced a catalog of such swarms in subduction zones, based on visual inspection of seismicity. *Zaliapin and Ben-Zion* [2013a, 2013b] developed a clustering method to isolate swarm activity but used a priori fixed model parameters, without testing the ability of the model in presence of a nonstationary background rate. *Reverso et al.* [2015] developed a method, extending the approach of *Marsan et al.* [2013], to measure the significance level of suspected episodes of aseismic deformation, based on a data-driven parameterized seismicity model.

In subduction zones, while seismic swarms can therefore be detected systematically, and potentially associated to SSEs, the question remains as to whether they can help in measuring the associated total slip. In effect, only numbers of anomalous earthquakes can be deduced from these methods. How these numbers can be translated into slow slip is still not understood, especially as the seismic moment relaxed by accompanying earthquakes is typically only a very small part of the total seismic moment relaxed by the SSE, similarly to aftershocks and postseismic slip following main shocks [*Shcherbakov et al.*, 2004; *Kagan and Houston*, 2005; *Perfettini and Avouac*, 2007].

We here investigate the relationship between changes in earthquake rate and aseismic slip, for the Boso area in Japan. SSEs in Boso (see Supporting Information S1) are known to occur repeatedly [*Ozawa et al.*, 2007; *Ozawa*, 2014; *Kato et al.*, 2014; *Hirose et al.*, 2014; *Fukuda et al.*, 2014]. They are associated with aseismic slip at the Philippine Sea plate-Okhotsk plate boundary. Slip has been inferred from geodetic measurements and

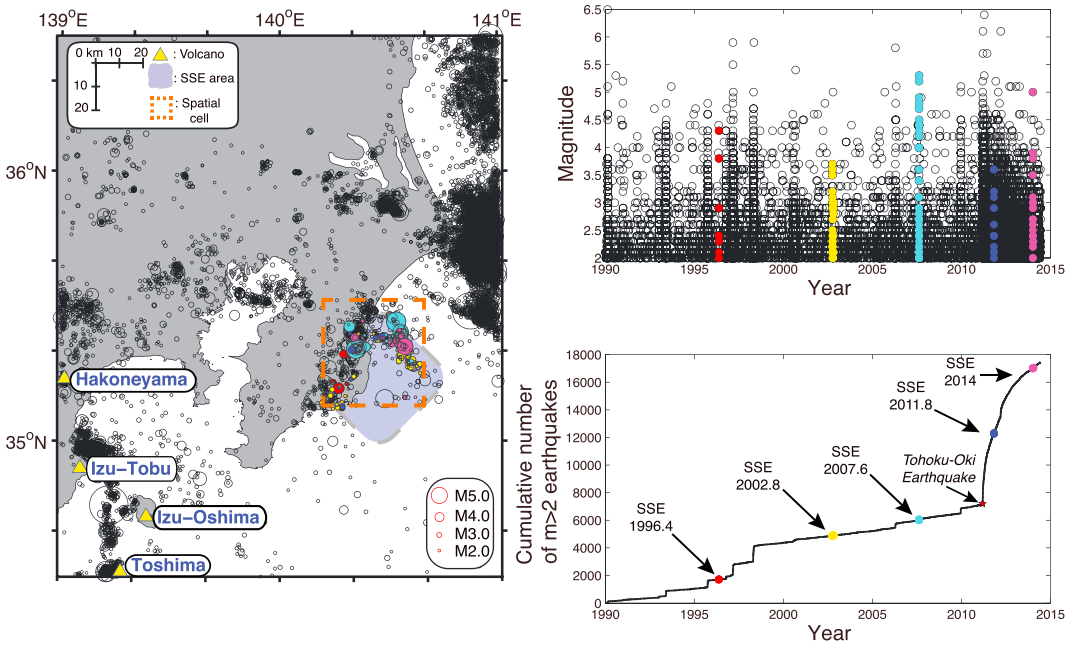


**Figure 1.** Map of the Boso area. We select earthquakes with depths smaller than 40 km, from 1 January 1990 to 12 June 2014. Five known episodes of SSEs have taken place during this period. Filled circles represent earthquakes occurring during these SSEs and are detected as abnormal using the method of *Reverso et al.* [2015]. The fault patch that repeatedly slip during SSE is outlined in blue. We here study the seismicity rate of the spatial cell delimited by the thick orange dashed lines.

affect a patch common to all known instances of SSEs that have occurred since 1996, with a surface of roughly $40 \times 40$ km$^2$, over typically 10 days. Coupling is found to be high on this patch during inter-SSE periods [*Sagiya*, 2004]. About 10 cm of slip is accommodated during each SSE; a mean waiting time of about 5 years between consecutive SSEs thus implies that most, if not all, of the 2.3 cm/yr convergence rate in Boso [*Nishimura et al.*, 2007] is effectively accommodated by this simple stick-slip process. Because they are shallow, these SSEs are associated with seismic swarms, located at the edges of the slipping patch, and displayed a similar, relatively isolated geographical pattern each time. *Ozawa et al.* [2007] calculated the energy released by these swarms and obtained a total moment of the order of 1% of the SSE moments, indicating that slow slip is the first process driving these earthquake swarms. The fact that several instances of well-documented SSEs activated the same fault patch and that they always trigger a similar pattern of seismicity observed by one of the best seismic networks in the world, make Boso a unique place to conduct our study. Moreover, this patch marks the eastern end of the locked portion of the Philippine Sea plate located underneath Tokyo, and a better understanding of the mechanical properties of this area is therefore of particular importance.

## 2. Data

We use the Japan Meteorological Agency seismic catalog for a period from the 1 January 1990 to 12 June 2014, for latitudes from 34.5° to 36.5°N and longitudes from 139° to 141°E (see Figure 1).

In the Boso Peninsula, the SSEs are located at the Eurasian and Philippine Sea plate interface, and the associated seismicity is located between 20 and 30 km depth [*Ozawa*, 2003; *Ozawa et al.*, 2007]. However, the 1996 and 2002 swarms have earthquakes between 30 and 40 km depth, very possibly due to uncertainties in the depth estimate. Consequently, we decide to keep earthquakes with depth less than 40 km. We estimate the magnitude of completeness at $m_c = 2.0$ for this data set (see Figure S1), which gives us a total of $N = 17,439$ earthquakes. We further note that the catalog is effectively complete at $m \geq 2.0$ during SSEs, see Figure S2. We detail in the supporting information, section 2, the characteristics of the SSEs at Boso, as described by other studies.

## 3. Method

The method proposed by *Reverso et al.* [2015] amounts to remove triggered earthquakes (i.e., aftershocks) from the data, by a probabilistic declustering that makes use of the time spans and distances between earthquakes. It is based on the probabilistic separation between two components, i.e., the background seismicity, which is the part of the seismicity due to aseismic processes, and the seismicity that corresponds to earthquakes triggered by other earthquakes.

The main assumption of this method is that earthquake sequences which cannot be explained by "normal" seismic triggering are modeled by an increase of the background seismicity. This separation is performed using the space-time ETAS model, which represents earthquakes as points occurring with rate-density $\lambda(x, y, t)$, defined as the mean number of earthquakes per unit area and unit time:

$$\lambda(x, y, t) = \mu(x, y, t) + \nu(x, y, t) \tag{1}$$

with $\mu(x, y, t)$, the background seismicity and $\nu(x, y, t)$, the rate density of triggered earthquakes. The latter term is modeled as the product of a temporal and spatial kernels

$$\nu(x, y, t) = \sum_{i|t_i<t} \nu_i(x, y, t) \tag{2}$$

with

$$\nu_i(x, y, t) = \frac{\kappa(m_i)}{(t + c - t_i)^p} \times \frac{(\gamma - 1)L(m_i)^{\gamma-1}}{2\pi\left((x - x_i)^2 + (y - y_i)^2 + L(m_i)^2\right)^{(\gamma+1)/2}} \tag{3}$$

where the summation in equation (2) is done for all earthquakes $i$ of magnitude $m_i$ occurring at time $t_i < t$ and location $(x_i, y_i)$, cf. also *Marsan et al.* [2013]. Here $c$, $\gamma$, and $p$ are model parameters, $L(m)$ and $\kappa(m)$ represent the rupture radius and the productivity law, respectively [*Ogata*, 1988; *Zhuang et al.*, 2005]. The productivity law $\kappa(m)$ is defined as $\kappa(m) = \kappa_0 \times e^{\alpha(m-m_c)}$ where $\kappa_0$ and $\alpha$ are model parameters and $m_c$ is the magnitude threshold. The rupture length $L$ scales with magnitude according to $L(m) = L_0 \times 10^{0.5(m-m_c)}$ where $L_0$ is the rupture radius for an earthquake of magnitude $m_c$, taken here as a parameter.

The model is first fit to the data by assuming $\mu$ to be constant in time but variable in space, hence, $\mu(x, y)$. The background seismicity $\mu(x, y)$ is computed with a smoothing length $\mathcal{L}$ defined arbitrarily [*Reverso et al.*, 2015]. In this first step, parameters $\alpha, p, c, K_0, L_0, \gamma$ and the background seismicity $\mu(x, y)$ are estimated together using an Expectation-Maximization algorithm. Namely, we first give an a priori (nonzero) guess of $\mu(x, y)$, typically assuming a uniform field (whose value, as long as it is nonzero, matters not). (i) Given $\mu(x, y)$, we optimize the parameters $\alpha, p, c, K_0, L_0, \gamma$, here using a simplex method; (ii) Expectation: Given these parameters and $\mu(x, y)$, the background probabilities are computed for each earthquake $i$ as $\omega_i = \frac{\mu(x_i,y_i)}{\mu(x_i,y_i)+\nu(x_i,y_i,t_i)}$. (iii) Maximization: The a posteriori background field $\mu(x, y)$ is then obtained by smoothing these probabilities with the smoothing length $\mathcal{L}$, here using a Gaussian kernel. We iterate steps (i) to (iii) until convergence of all parameters and $\mu(x, y)$.

Focusing on the specific area where swarms occur, i.e., for latitudes from 35.15° to 35.51° and longitudes from 140.18° to 140.62°, we compute the local stationary background rate $\mu_{xy}$. The log likelihood is $\ell = -TS\mu_{xy} + \sum_j \ln(\nu_j + \mu_{xy})$, where $j$ represents all the earthquakes occurring in this geographical box of surface $S$, and $T$ is the duration of the catalog. The Maximum Likelihood Estimator (MLE) is then given by

$$TS - \sum_j \frac{1}{(\mu_{xy} + \nu_j)} = 0 \tag{4}$$

Likewise, the time-varying background rate $\mu_{xyt}$ can be estimated with the MLE for nonoverlapping time windows of duration $\tau$ as

$$\tau S - \sum_j \frac{1}{(\mu_{xyt} + \nu_j)} = 0 \tag{5}$$

the summation now being done on all earthquakes $j$ in the geographical box and in the time window considered. We finally quantify the significance of the difference in log likelihood between the stationary and the nonstationary background models using a Monte Carlo method, see *Reverso et al.* [2015] for details.

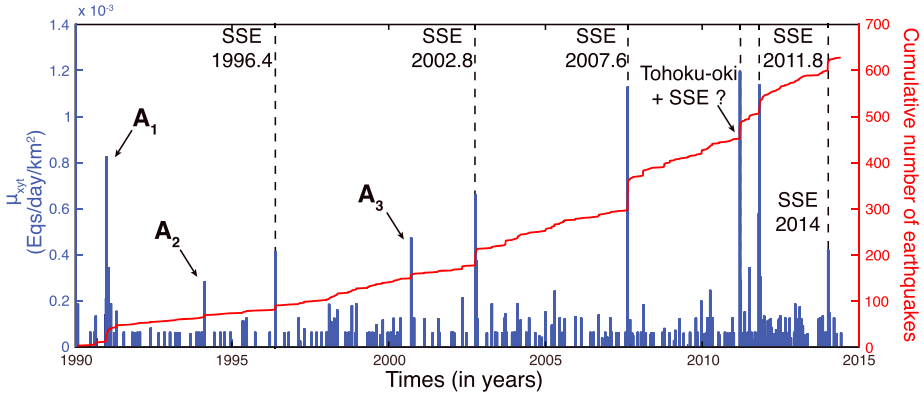


**Figure 2.** Cumulative number of earthquakes (in red) and time series of the background seismicity rate $\mu_{xyt}$ (in blue) for the Boso area. The three transients occurring outside the five known SSEs are labeled $A_1$, $A_2$, and $A_3$.

## 4. Relationship Between Slow Slip and Background Seismicity

Inversion of the model parameters, for $\mathcal{L}=40$ km, gives $p=1.132$, $c=0.002$ days, $L_0=0.099$ km (for $m_c=2.0$), $\gamma=2.339$, and $K_0=0.006$. We fix $\alpha$ to 2.0, otherwise the inverted $\alpha$ value is low (<1.0). It is known that seismicity dominated by swarms cause the estimated $\alpha$ to yield unrealistic low values [*Hainzl et al.*, 2013]. Moreover, with a too low $\alpha$ value, the model becomes more flexible and able to adjust to sudden variations in the time series, preventing it to detect abnormal seismic activity in the data. The nonstationary background rate is then computed using $\tau = 10$ days. We show, in Figure 2, the cumulative number of earthquakes and the time series of the background seismicity rate-density $\mu_{xyt}$ calculated for the $40 \times 40$ km$^2$ cell of Figure 1. SSEs are clearly marked by large values of $\mu_{xyt}$, although the most important increase is found in 2011.2, right after the 2011 $M_w$9.0 Tohoku-Oki earthquake. The widespread activation of seismicity following this shock included the eastern part of our study area [*Hirose et al.*, 2011; *Ishibe et al.*, 2011; *Toda et al.*, 2011; *Toda and Stein*, 2013]. The high increase of background seismicity is produced because the Tohoku-Oki earthquake is located outside the studied area (i.e., Kanto region). It is therefore absent from our catalog; the triggering term $\nu$ thus cannot explain this increase in earthquake activity, which is therefore included in the background term. Other peaks in background rates are discussed in the supporting information.

The anomalous sequences detected during known SSE episodes are listed in Table 1. All these anomalies are very significant, with probabilities to be abnormally greater than 95%. We note that the numbers of earthquakes occurring during these swarms are only weakly correlated with the moments of the SSEs (Figure 3a), while the increases $\frac{\mu_{xyt}}{\mu_{xy}}$ in background rate are at 0.96 (increasing to 0.97 if further requiring that $\mu_{xyt}=0$ for $M_{SSE}=0$), see Figure 3b. This correlation is in agreement with the linear relationship found at large scale for subduction zones [*Ide*, 2013]. We estimate the best linear trend $M_{SSE} = a \times 10$ days $\times \frac{\mu_{xyt}}{\mu_{xy}}$ with $a=2.431 \pm 0.078 \times 10^{16}$ N m d$^{-1}$. This coefficient $a$ is equivalent to the long-term seismic moment rate $\dot{M}_{LT}$,

**Table 1.** Earthquake Swarms Detected by Our Model for $\mathcal{L} = 40$ Km and $\tau = 10$ Days, at the Time of Known SSEs[a]

| Date (years) | Numbers of $m \geq 2$ Earthquakes | Ratio $\mu_{xyt}/\mu_{xy}$ | Probability to Be Anomalous |
|---|---|---|---|
| 1996.4 | 10 | 18.3 | >99.99% |
| 2002.8 | 29 | 29.1 | 99.94% |
| 2007.6 | 63 | 49.9 | 99.94% |
| 2011.8 | 22 | 50.3 | >99.99% |
| 2014 | 21 | 18.6 | 97.3% |

[a]We note that all swarms are detected with very high significance levels.

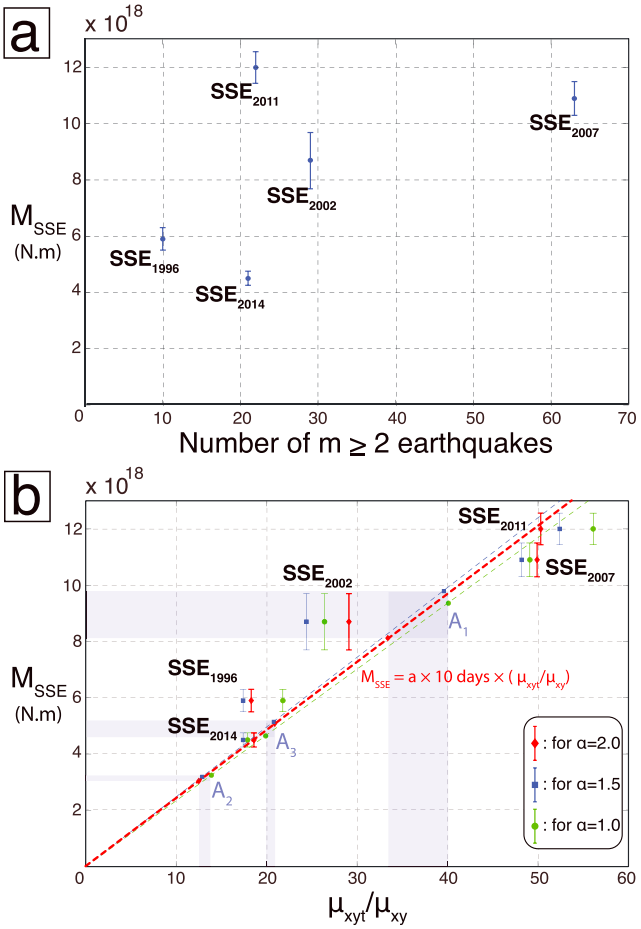


**Figure 3.** (a) Seismic moment relaxed during the SSEs versus the number of $m \geq 2.0$ earthquakes occurring at the same time in the cell of Figure 1. The coefficient of correlation is $\rho = 0.53$, due to the fact that we count all earthquakes in the cell, including aftershocks. (b) Relationship between the increases in background rate-density $\frac{\mu_{xyt}}{\mu_{xy}}$ and seismic moment of the SSEs (for a common duration of 10 days for all SSEs) using different $\alpha$ values (1.0, 1.5, and 2.0). For the best fit, i.e, $\alpha = 2.0$, the two quantities are correlated at $\rho = 0.96$; we display the best linear fit $M_{SSE} = a \times 10$ days $\times \frac{\mu_{xyt}}{\mu_{xy}}$, obtained for $a = 2.431 \pm 0.078 \times 10^{16}$ N m d$^{-1}$.

since the moment release rate is equal to $a$ when $\frac{\mu_{xyt}}{\mu_{xy}} = 1$, i.e., over long time scales. It gives a yearly rate equal to $8.88 \times 10^{18}$ N m yr$^{-1}$. In the seismic moment relationship [*Aki*, 1966]

$$\dot{M}_{LT} = G \times S \times D \tag{6}$$

with a rigidity modulus $G$ of 30 GPa and a surface $S$ of $40 \times 40$ km$^2$, we infer a long-term (over nearly 25 years) displacement rate of $0.185 \pm 0.006$ m/yr. We tested the sensibility of our results with $\alpha$, by rerunning our analysis for $\alpha = 1.0$ and $\alpha = 1.5$. We found a long-term displacement of 0.178 and $0.18 \pm 0.006$ m/yr for these two cases, but with a lower correlation between the increases in background seismicity and the seismic moments of the SSEs (0.942 and 0.949, for $\alpha = 1.5$ and $\alpha = 1.0$, respectively), see Figure 3b.

This slip rate becomes 0.201 m/yr when keeping $m \geq 1.5$ earthquakes, and 0.161 m/yr for $m \geq 3.0$, cf. Figure S3 in the supporting information. This estimate is thus robust regarding the changes in both $\alpha$ and $m_c$.

Our long-term slip rate is estimated for a 25 year long period that covers several phases of co- and inter-SSE periods. *Nishimura et al.* [2007] suggested a total coupling in this region during inter-SSE phases, along with a convergence rate of 23 mm/yr. In the case where shear is totally relaxed in Boso during SSEs, i.e., there is full coupling during inter-SSE phases and full uncoupling during SSEs, the slip rate over the 1990–2014 period should equal the long-term convergence rate estimated at 23 mm/yr [*Nishimura et al.*, 2007]. Our estimate is 8 times higher, implying that the gains $\frac{\mu_{xyt}}{\mu_{xy}}$ during SSEs would be underestimated by a factor of 8 if our

argument were valid. This discrepancy likely comes from the fact that the slip causing earthquakes to occur in this area is different in the inter-SSE and the co-SSE phases, both in duration and in location: seismicity is driven during SSEs by slip on the SSE patch, and during inter-SSE periods by slip downdip on this patch, as coupling is estimated to be complete above 20 km depth. We here examine these two differences.

A first explanation is that $\mu$ evolves in time more slowly than does the slip rate, as expected with rate-and-state friction [*Dieterich*, 1994; *Dieterich et al.*, 2000], which predicts that a sudden change in stressing rate $\dot{\tau}$ from $\dot{\tau}_0$ to $\dot{\tau}'_0 = x \times \dot{\tau}_0$ (gain $x$) at time $t = 0$ will cause the rate of earthquakes to increase from $\mu$ to $\frac{\mu x}{1+(x-1)e^{-t/t'_a}}$ where $t'_a = \frac{t_a}{x} = \frac{A\sigma}{x\dot{\tau}_0}$ is a characteristic time. For a gain in rate $\mu$ to be 8 times less than the gain in stressing rate $\dot{\tau}$, after a typical time of 10 days, it is required that $t'_a = \frac{t_a}{x} \simeq \frac{10}{\ln(x/7)}$ days (assuming $x \gg 1$). This equation relates two quantities that are largely unknown:

1. $t_a$, the characteristic relaxation time, was estimated to 2 years for the Kanto region [*Toda and Stein*, 2013]. This parameter $t_a$ is typically of the order of years when analyzing regional earthquake catalogs.
2. The relative increase $x = \frac{\dot{\tau}'_0}{\dot{\tau}_0}$ in stressing rate $\dot{\tau}$ (or, equivalently, in slipping rate $\dot{\delta}$) suffers from the lack of resolution of the inter-SSE slipping rate.

According to *Nishimura et al.* [2007], it could amount to about 12 mm/yr, i.e., the difference between the modeled slip rate of 42 mm/yr and the estimated 30 mm/yr inferred from SSE return times, see paragraph [40] of *Nishimura et al.* [2007]. For a typical slip of ≃20 cm over 10 days during a typical SSE [*Ozawa*, 2014], the ratio $x$ equals 600. Since the mean gain of seismicity rate $\frac{1}{t}\int_0^t dt' \frac{x}{1+(x-1)\exp(-t'/t'_a)} = \frac{t'_a}{t} x \ln\left(1 + \frac{\exp(t/t'_a)-1}{x}\right)$ equals $x/8$ after $t = 10$ days, we obtain that $t'_a = 1.50$ days, which would give $t_a = x \times t'_a = 2.4$ years, yielding a plausible estimate of $t_a$. This shows that the apparent overestimation of the long-term slip rate inferred from SSEs, using our method, is coherent with a rate-and-state friction model of the Boso area.

A second explanation is related to the different locations of the two slip sources. As stress change decays inversely to the cube of the distance, a factor of 8 is equivalent to locating the centroid of the inter-SSE slip about half as far as the barycenter of the co-SSE slip. Since the latter is at about 25–30 km from the seismicity swarm [*Hirose et al.*, 2014; *Ozawa*, 2014], this implies that the transition from full coupling to full uncoupling is relatively sharp, i.e., over distances less than 15 km, hence with full uncoupling starting at depths of about 25 km.

## 5. Long-Term Acceleration

SSEs in Boso have been occurring with shorter and shorter recurrence intervals since 1996 [*Ozawa*, 2014]. In particular, the 2014 SSE followed the October 2011 SSE by only 2.2 years, so significantly less than the typical 4 and 6 year long intervals for preceding SSEs. Whether this shortening is mostly due to the 2011 $M_w$9.0 Tohoku-Oki earthquake and more particularly its postseismic slip [*Hirose et al.*, 2012], or to a much longer process taking place over years and independent of the 2011 shock, is unknown. *Ozawa* [2014] suggested that it could indeed mark the nearing of the end of a slip cycle in the Sagami Trough, as confirmed by friction models [e.g., *Mitsui*, 2015].

Earthquake activity has accelerated over the last 25 years in the Boso area. Figure S4 shows that a quadratic polynomial fit can account for the observed acceleration, at magnitude cutoffs 1.5, 2.0, and 3.0, making this observation robust. We also observe a similar quadratic acceleration for the background rate $\mu_{xyt}$; using the relationship of Figure 3b, keeping a rigidity of 30 GPa, and taking into account the $\frac{1}{8}$ proportionality factor between the estimated slip rate and the true slip rate (for 10 day long intervals, see Supporting Information S1), we infer that the inter-SSE slip rate in the Boso area has also been accelerating at a rate of 1.1 mm/yr/yr since 1990, see Figure 4. This acceleration reduces to 1.0 mm/yr/yr when removing the transient increases in background rate related to swarms $A_1$, $A_2$, and $A_3$, and to the immediate effect of the 2011 Tohoku-Oki earthquake.

Interestingly, we find that the recurrence intervals between the 1996, 2002, 2007, and 2011 SSEs correspond to the accumulation of 11.4 ± 0.3 cm of our estimated slip each time. The 2014 SSE is an exception to this rule, since only 6.8 cm accumulated between the 2011 and the 2014 SSE. A local maximum of postseismic slip following the 2011 Tohoku earthquake is found near Boso, although its exact location is uncertain [*Ozawa et al.*, 2012; *Perfettini and Avouac*, 2014]; it is therefore likely that extra forcing on the seismicity-prone area of Boso

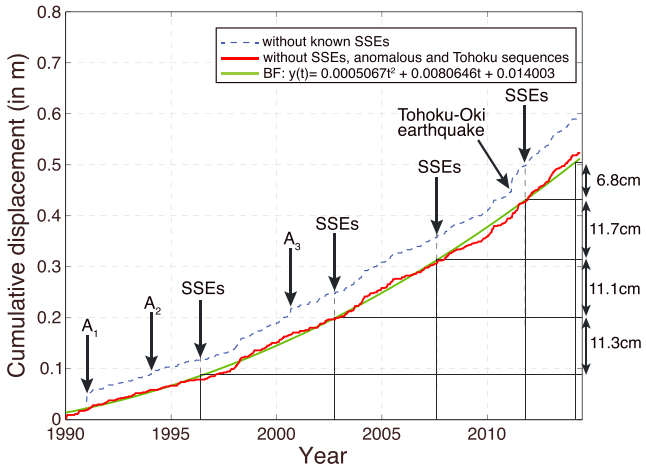


**Figure 4.** Inferred displacement at Boso, using our estimated background rate, and the relationship of Figure 3. The dashed curve is obtained after removing the SSEs; the thick curve has also the transients $A_1$-$A_3$ and the direct effect of the 2011 Tohoku-Oki earthquake removed. The best quadratic polynomial fit is shown. It yields a fixed displacement of 11.4 cm between the 1996, 2002, 2007 and 2011 SSEs.

caused a clock advance for the 2014 SSE, as already suggested for the 2011 SSE by *Hirose et al.* [2012]. This suggests that slow slip events in Boso are indeed related to a simple threshold (stick-slip) mechanism. Seismicity in Boso therefore results from both (i) inter-SSE phases, as the loosely coupled downdip extension of the Philippine Sea plate slab interface forces the transitional zone delimiting the base of the locked SSE-prone patch, and (ii) the co-SSE phase that causes the background seismicity rate to increase by a factor of 10 to 50 (Figure 3b) over 10 days. The long-term acceleration of seismicity described here is thus likely due to a slow uncoupling downdip in the SSE patch, i.e., at depths larger than 20 km or equivalently to an updip migration of the top of the fully uncoupled slip interface at depth, i.e., a shrinking of the transitional zone. With this model, the shortening of inter-SSE intervals of *Ozawa* [2014] is a natural consequence of the acceleration of the displacement rate of Figure 4, which clearly predates the occurrence of the 2011 Tohoku-Oki earthquake. It is therefore likely that the Boso area is indeed slowly decoupling at depth (possibly via a shrinking of the transitional zone), increasing the stress transfer rate to neighboring locked patches of the Philippine Sea plate slip interface, especially in the Sagami Trough which has not ruptured since the 1703 Genroku Kanto earthquake.

## 6. Conclusion

We found a linear relationship between the seismic moment relaxed by SSEs in Boso and the change in background seismicity rate, estimated from a seismicity model of the wider Kanto region at shallow depth. This proportionality is in agreement with a similar finding by *Ide* [2013] who related plate velocity and background rate in subduction zones. The present analysis shows that this proportionality exists also at small (~40 km) scale and holds even during slow deformation transients. Moreover, friction modeling, although difficult to parameterize accurately, can explain the modest gain in background seismicity rate during SSEs, relative to what would be expected if background activity were to follow changes in slip rate without any delay. This method has therefore the potential to provide indirect estimates of the slip rate during slow slip events, without the use of geodetic data, even at depths where slow slip manifests itself through swarms of low to very low frequency earthquakes [*Shelly et al.*, 2007; *Frank et al.*, 2015; *Ghosh et al.*, 2015]. However, since the linear relationship is based on a limited sample (only five SSEs, in addition to the constraint that $\mu_{xyt} = 0$ if $M_{SSE} = 0$), we must stress that future observations of SSEs are required to fully validate and calibrate this proportionality.

Acceleration of slip in the Boso area is found to occur steadily over the 1990–2014 period, with a rate of +1.0 mm/yr/yr. This acceleration can explain the observation by *Ozawa* [2014] that SSEs occur with shorter recurrent intervals, if SSEs are triggered each time the accumulated slow slip has reached a total displacement of 11.4 ± 0.3 cm. This long-term acceleration in Boso thus predates the occurrence of the 2011 Tohoku earthquake, and could mark the slow uncoupling at depth ($z > 20$ km) potentially related to the nearing of the seismic cycle of the easternmost locked portion of the Philippine Sea plate.

**Acknowledgments**
This work was financially supported by the EC REAKT and MARSITE projects. We used the earthquake catalog arranged by the Japan Meteorological Agency in cooperation with the Ministry of Education, Culture, Sports, Science and Technology. Bogdan Enescu is supported by JSPS KAKENHI grant 26240004. We thank the two anonymous referees for their constructive comments and suggestions.

## References

Aki, K. (1966), Generation and propagation of G waves from the Niigata earthquake of June 16, 1964. Part 2. Estimation of earthquake moment, released energy, and stress-strain drop from G wave spectrum, *Bull. Earthquake Res. Inst. Tokyo Univ.*, *44*, 73–88.

Delahaye, E. J., J. Townend, M. E. Reyners, and G. Rogers (2009), Microseismicity but no tremor accompanying slow slip in the Hikurangi subduction zone, New Zealand, *Earth Planet. Sci. Lett.*, *277*, 21–28.

Dieterich, J. (1994), A constitutive law for rate of earthquake production and its application to earthquake clustering, *J. Geophys. Res.*, *99*, 2601–2618.

Dieterich, J., V. Cayol, and P. Okubo (2000), The use of earthquake rate changes as a stressmeter at Kilauea volcano, *Nature*, *408*, 457–460.

Frank, W. B., M. Radiguet, B. Rousset, N. M. Shapiro, A. L. Husker, V. Kostoglodov, N. Cotte, and M. Campillo (2015), Uncovering the geodetic signature of silent slip through repeating earthquakes, *Geophys. Res. Lett.*, *42*, 2774–2779, doi:10.1002/2015GL063685.

Fukuda, J., A. Kato, K. Obara, S. Miura, and T. Kato (2014), Imaging of the early acceleration phase of the 2013–2014 Boso slow slip event, *Geophys. Res. Lett.*, *41*, 7493–7500, doi:10.1002/2014GL061550.

Ghosh, A., E. Huesca-Pérez, E. Brodsky, and Y. Ito (2015), Very low frequency earthquakes in Cascadia migrate with tremor, *Geophys. Res. Lett.*, *42*, 3228–3232, doi:10.1002/2015GL063286.

Hainzl, S., O. Zakharova, and D. Marsan (2013), Impact of aseismic transients on the estimation of aftershock productivity parameters, *Bull. Seismol. Soc. Am.*, *103*, 1723–1732.

Hirose, F., K. Miyaoka, N. Hayashimoto, T. Yamazaki, and M. Nakamura (2011), Outline of the 2011 off the Pacific coast of Tohoku Earthquake ($M_w$ 9.0)—Seismicity: Foreshocks, mainshock, aftershocks, and induced activity, *Earth Planet Space*, *63*, 513–518.

Hirose, H., H. Kimura, B. Enescu, and S. Aoi (2012), Recurrent slow slip event likely hastened by the 2011 Tohoku earthquake, *Proc. Natl. Acad. Sci. U.S.A.*, *109*, 15,157–15,161.

Hirose, H., T. Matsuzawa, T. Kimura, and H. Kimura (2014), The Boso slow slip events in 2007 and 2011 as a driving process for the accompanying earthquake swarm, *Geophys. Res. Lett.*, *41*, 2778–2785, doi:10.1002/2014GL059791.

Holtkamp, S. G., and M. R. Brudzinski (2011), Earthquake swarms in circum-Pacific subduction zones, *Earth Planet. Sci. Lett.*, *305*, 215–225.

Ide, S. (2013), The proportionality between relative plate velocity and seismicity in subduction zones, *Nat. Geosci.*, *6*, 780–784.

Ishibe, T., K. Shimazaki, K. Satake, and H. Tsuruoka (2011), Change in seismicity beneath the Tokyo metropolitan area due to the 2011 off the Pacific coast of Tohoku earthquake, *Earth Planet Space*, *63*, 731–735.

Kagan, Y. Y., and H. Houston (2005), Relation between mainshock rupture process and Omori's law for aftershock moment release rate, *Geophys. J. Int.*, *163*, 1039–1048.

Kato, A., T. Igarashi, and K. Obara (2014), Detection of a hidden Boso slow slip event immediately after the 2011 $M_w$ 9.0 Tohoku-Oki earthquake, Japan, *Geophys. Res. Lett.*, *41*, 5868–5874, doi:10.1002/2014GL061053.

Liu, Y., J. R. Rice, and K. M. Larson (2007), Seismicity variations associated with aseismic transients in Guerrero, Mexico, 1995-2006, *Earth Planet. Sci. Lett.*, *262*, 493–504.

Marsan, D., T. Reverso, A. Helmstetter, and B. Enescu (2013), Slow slip and aseismic deformation episodes associated with the subducting Pacific plate offshore Japan, revealed by changes in seismicity, *J. Geophys. Res. Solid Earth*, *118*, 4900–4909, doi:10.1002/jgrb.50323.

Mitsui, Y. (2015), Interval modulation of recurrent slow slip events by two types of earthquake loading, *Earth Planet Space*, *67*, 1–8.

Montgomery-Brown, E. K., P. Segall, and A. Miklius (2009), Kilauea slow slip events: Identification, source inversions, and relation to seismicity, *J. Geophys. Res.*, *114*, B00A03, doi:10.1029/2008JB006074.

Montgomery-Brown, E. K., D. K. Sinnett, K. M. Larson, M. P. Poland, P. Segall, and A. Miklius (2011), Spatiotemporal evolution of dike opening and décollement slip at Kīlauea Volcano, Hawai'i, *J. Geophys. Res.*, *116*, B03401, doi:10.1029/2010JB007762.

Montgomery-Brown, E. K., C. H. Thurber, C. J. Wolfe, and P. Okubo (2013), Slow slip and tremor search at Kilauea Volcano, Hawaii, *Geochem. Geophys. Geosyst.*, *14*, 367–384, doi:10.1002/ggge.20044.

Nishimura, T., T. Sagiya, and R. S. Stein (2007), Crustal block kinematics and seismic potential of the northernmost Philippine Sea plate and Izu microplate, central Japan, inferred from GPS and leveling data, *J. Geophys. Res.*, *112*, B05414, doi:10.1029/2005JB004102.

Ogata, Y. (1988), Statistical models for earthquake occurrences and residual analysis for point processes, *J. Am. Stat. Assoc.*, *83*, 9–27.

Ozawa, S. (2003), Characteristic silent earthquakes in the eastern part of the Boso peninsula, Central Japan, *Geophys. Res. Lett.*, *30*(6), 1283, doi:10.1029/2002GL016665.

Ozawa, S. (2014), Shortening of recurrence interval of Boso slow slip events in Japan, *Geophys. Res. Lett.*, *41*, 2762–2768, doi:10.1002/2014GL060072.

Ozawa, S., H. Suito, and M. Tobita (2007), Occurrence of quasi-periodic slow-slip off the east coast of the Boso peninsula, Central Japan, *Earth Planet Space*, *59*, 1241–1245.

Ozawa, S., T. Nishimura, H. Munekane, H. Suito, T. Kobayashi, M. Tobita, and T. Imakiire (2012), Preceding, coseismic, and postseismic slips of the 2011 Tohoku earthquake, Japan, *J. Geophys. Res.*, *117*, B07404, doi:10.1029/2011JB009120.

Perfettini, H., and J. P. Avouac (2007), Modeling afterslip and aftershocks following the 1992 Landers earthquake, *J. Geophys. Res.*, *112*, B07409, doi:10.1029/2006JB004399.

Perfettini, H., and J. P. Avouac (2014), The seismic cycle in the area of the 2011 $M_w$ 9.0 Tohoku-Oki earthquake, *J. Geophys. Res. Solid Earth*, *119*, 4469–4515, doi:10.1002/2013JB010697.

Reverso, T., D. Marsan, and A. Helmstetter (2015), Detection and characterization of transient forcing episodes affecting earthquake activity in the Aleutian Arc system, *Earth Planet. Sci. Lett.*, *412*, 25–34.

Sagiya, T. (2004), Interplate coupling in the Kanto District, Central Japan, and the Boso Peninsula silent earthquake in May 1996, *Pure Appl. Geophys.*, *161*, 2327–2342.

Shcherbakov, R., D. L. Turcotte, and J. B. Rundle (2004), A generalized Omori's law for earthquake aftershock decay, *Geophys. Res. Lett.*, *31*, L11613, doi:10.1029/2004GL019808.

Shelly, D. R., G. C. Beroza, and S. Ide (2007), Non-volcanic tremor and low-frequency earthquake swarms, *Nature*, *446*, 305–307.

Toda, S., and R. S. Stein (2013), The 2011 $M = 9.0$ Tohoku Oki earthquake more than doubled the probability of large shocks beneath Tokyo, *Geophys. Res. Lett.*, *40*, 2562–2566, doi:10.1002/grl.50524.

Toda, S., R. S. Stein, and J. Lin (2011), Widespread seismicity excitation throughout central Japan following the 2011 $M = 9.0$ Tohoku earthquake and its interpretation by Coulomb stress transfer, *Geophys. Res. Lett.*, *38*, LG00G03, doi:10.1029/2011GL047834.

Vallée, M., et al. (2013), Intense interface seismicity triggered by a shallow slow slip event in the Central Ecuador subduction zone, *J. Geophys. Res. Solid Earth*, *118*, 2965–2981, doi:10.1002/jgrb.50216.

Vidale, J. E., A. J. Hotovec, A. Ghosh, K. C. Creager, and J. Gomberg (2011), Tiny intraplate earthquakes triggered by nearby episodic tremor and slip in Cascadia, *Geochem. Geophys. Geosyst.*, *12*, Q06005, doi:10.1029/2011GC003559.

Zaliapin, I., and Y. Ben-Zion (2013a), Earthquake clusters in southern California I: Identification and stability, *J. Geophys. Res. Solid Earth*, *118*, 2847–2864, doi:10.1002/jgrb.50179.

Zaliapin, I., and Y. Ben-Zion (2013b), Earthquake clusters in southern California II: Classification and relation to physical properties of the crust, *J. Geophys. Res. Solid Earth*, *118*, 2865–2877, doi:10.1002/jgrb.50178.

Zhuang, J., C. P. Chang, Y. Ogata, and Y. I. Chen (2005), A study on the background and clustering seismicity in the Taiwan region by using point process models, *J. Geophys. Res.*, *110*, B05S18, doi:10.1029/2004JB003157.